

Aggregation Behavior of Long-Chain *N*-Aryl Imidazolium Bromide in Aqueous SolutionLijuan Shi,<sup>†</sup> Na Li,<sup>‡</sup> Han Yan,<sup>†</sup> Yan'an Gao,<sup>†</sup> and Liqiang Zheng<sup>\*†</sup><sup>†</sup>Key Laboratory of Colloid and Interface Chemistry, Shandong University, Ministry of Education, Jinan 250100, China, and <sup>‡</sup>College of Chemistry, Chemical Engineering and Materials Science, Shandong Normal University, Jinan 250014, China

Received September 13, 2010

The aggregation behavior of three long-chain *N*-aryl imidazolium ionic liquids (ILs), 1-(2,4,6-trimethylphenyl)-3-alkylimidazolium bromide [C<sub>*n*</sub>pim]Br (*n* = 10, 12, and 14), in aqueous solutions was systematically explored by surface tension, electrical conductivity, and <sup>1</sup>H NMR. A lower critical micelle concentration (cmc) for the *N*-aryl imidazolium ILs is observed compared with that for 1,3-dialkylimidazolium ILs [C<sub>*n*</sub>mim]Br, indicating that the incorporation of the 2,4,6-trimethylphenyl group into a headgroup favors micellization. The enhanced  $\pi$ - $\pi$  interactions among the adjacent 2,4,6-trimethylphenyl groups weaken the steric hindrance of headgroups and thus lead to a dense arrangement of [C<sub>*n*</sub>pim]Br molecules at the air-water interface. An analysis of the <sup>1</sup>H NMR spectra revealed that the introduced 2,4,6-trimethylphenyl group may slightly bend into the hydrophobic regions upon micellization. The micelle formation process for [C<sub>*n*</sub>pim]Br (*n* = 10, 12, and 14) was found to be enthalpy-driven in the investigated temperature range, which is attributed to the strong electrostatic self-repulsion of the headgroups and the counterions as well as the  $\pi$ - $\pi$  interactions among headgroups. Strong, stable fluorescence properties are presented by the new *N*-aryl imidazolium ILs, indicating their potential application in the field of photochemistry.

## Introduction

Ionic liquids (ILs), as a class of environmentally friendly solvents, have significantly developed recently because of their extraordinary properties such as nonvolatility, nonflammability, high stability, high ionic conductivity, and easy recyclability.<sup>1,2</sup> Numerous ILs based on imidazolium, pyridinium, and quaternary ammonium cations with a variety of anions such as halides, PF<sub>6</sub><sup>-</sup>, BF<sub>4</sub><sup>-</sup>, (CF<sub>3</sub>SO<sub>3</sub>)<sub>2</sub>N<sup>-</sup>, and CF<sub>3</sub>SO<sub>3</sub><sup>-</sup> have been successively synthesized and widely utilized in organic synthesis, catalysis, and the preparation of nanostructured materials.<sup>3-5</sup> Recently, task-specific ionic liquids have emerged, where functional groups are introduced as a part of the *N*-alkyl substituent to impart a particular capability to the ILs.<sup>6,7</sup> Even so, the development of ILs is generally confined to *N*-alkyl ILs (e.g., 1,3-dialkylimidazolium salts), which restricts the variation of characteristics and applications of ILs.<sup>8</sup>

Currently, attempts have been focused on the design and synthesis of *N*-aryl imidazolium ILs. The incorporation of aryl substituents into the nitrogen atoms of the heterocycle will significantly tune the properties of the cations, such as the size, polarity, and charge distribution, which allows a far greater variation of the IL characteristics than imagined in current systems. Kouwer et al.<sup>9</sup> first synthesized a series of imidazolium-based ionic liquid

crystals (ILCs) with extended aromatic cores, where gratifying properties of the novel ILCs, such as high thermal stabilities and strong fluorescence behaviors were presented. Then a series of aryl alkyl imidazolium-based ILs were designed by Ahrens et al.,<sup>10</sup> who demonstrated that the combination of sp<sup>3</sup> alkyl and sp<sup>2</sup> aryl substituents at the nitrogen atoms of the imidazolium core caused a remarkable modification of the physicochemical properties (e.g., lower melting points, higher decomposition temperatures) compared with those of current 1,3-dialkylimidazolium ILs. Most importantly, strong electronic and steric effects of the substituents on the aromatic ring of the imidazolium cations were also observed, indicating that the characteristics of *N*-aryl ILs can be further tuned because various substitution patterns with different functions are easy to graft onto the aromatic ring. Owing to the introduced  $\pi$  system and the possibility to interact with other substances through  $\pi$ - $\pi$  interactions, the application value of the new tunable aryl alkyl ionic liquids (TAAILs) in the areas of extraction separation, catalytic reaction, and self-assembled materials is significantly enhanced.<sup>9,10</sup>

Because of their unique chemical and physical properties, ILs have been extensively studied and widely used in the field of colloid and interface science in recent years. The aggregation behavior of imidazolium ILs in aqueous solution has been intensively explored.<sup>11-14</sup> Aggregation behavior in aqueous solutions of three imidazolium ILs, 1-butyl-3-methylimidazolium

\*Corresponding author. E-mail: lqzheng@sdu.edu.cn. Phone: +86-531-88366062. Fax: +86-531-88564750.

(1) Rogers, R. D.; Seddon, K. R. *Science* **2003**, *302*, 792-793.  
(2) Welton, T. *Chem. Rev.* **1999**, *99*, 2071-2084.  
(3) Song, C. E. *Chem. Commun.* **2004**, 1033-1043.  
(4) Zhao, D. B.; Wu, M.; Kou, Y.; Min, E. Z. *Catal. Today* **2002**, *74*, 157-189.  
(5) Wang, Y.; Yang, H. *J. Am. Chem. Soc.* **2005**, *127*, 5316-5317.  
(6) Chamot, B.; Rizzi, C.; Gaillon, L.; Sirieix-Plenet, J.; Lelievre, J. *Langmuir* **2009**, *25*, 1311-1315.  
(7) Li, N.; Fang, G.; Liu, B.; Zhang, J.; Zhao, L.; Wang, S. *Anal. Sci.* **2010**, *26*, 455-459.  
(8) Giernoth, R. *Top. Curr. Chem.* **2007**, *276*, 1-23.  
(9) Kouwer, P. H. J.; Swager, T. M. *J. Am. Chem. Soc.* **2007**, *129*, 14042-14052.

(10) Ahrens, S.; Peritz, A.; Strassner, T. *Angew. Chem., Int. Ed.* **2009**, *48*, 7908-7910.

(11) Goodchild, I.; Collier, L.; Millar, S. L.; Prokes, I.; Lord, J. C. D.; Butts, C. P.; Bowers, J.; Webster, J. R. P.; Heenan, R. K. *J. Colloid Interface Sci.* **2007**, *307*, 455-468.

(12) Bowers, J.; Butts, C. P.; Martin, P. J.; Vergara-Gutierrez, M. C. *Langmuir* **2004**, *20*, 2191-2198.

(13) Dong, B.; Li, N.; Zheng, L. Q.; Yu, L.; Inoue, T. *Langmuir* **2007**, *23*, 41784182.

(14) Dong, B.; Zhao, X. Y.; Zheng, L. Q.; Zhang, J.; Li, N.; Inoue, T. *Colloids Surf., A* **2008**, *317*, 666-672.

tetrafluoroborate ( $[\text{C}_4\text{mim}]\text{BF}_4$ ), 1-octyl-3-methylimidazolium chloride ( $[\text{C}_8\text{mim}]\text{Cl}$ ), and 1-octyl-3-methylimidazolium iodide ( $[\text{C}_8\text{mim}]\text{I}$ ), has been explored by Bowers et al.<sup>12</sup> Our group systematically investigated the surface properties and aggregation behavior of aqueous solutions of long-chain 1,3-dialkylimidazolium ILs  $\text{C}_n\text{mimBr}$  ( $n = 10, 12, 14$ , and 16) and 1-dodecyl-3-methylimidazolium tetrafluoroborate ( $[\text{C}_{12}\text{mim}]\text{BF}_4$ ).<sup>13,14</sup> In addition, much research has focused on the effect of structural change (especially the long hydrocarbon chain) on the aggregation behavior of ILs in water. For example, Firestone and co-workers<sup>15</sup> described the self-aggregation of thiophene-tailed imidazolium ILs in aqueous solutions. Our group synthesized a class of fluorescent carbazole-tailed imidazolium ILs and studied their aggregation behavior in water, where the incorporation of a carbazole moiety improved the ability of imidazolium ILs to form micelles.<sup>16</sup> However, few investigations have considered the effect of change in the polar head on the aggregation behavior of ILs in water. Yoshida et al.<sup>17</sup> reported that methylation at the 2-position of the imidazolium ring induces an increase in surface tension. For traditional cationic surfactants (e. g., cetyltrialkylammonium halides), the incorporation of an aromatic group into the headgroup produces interesting consequences, such as a lower cmc and equilibrium constant for micelle formation ( $K$ ).<sup>18,19</sup> The effect of the incorporated aromatic group on molecular aggregation, on one hand, is unfavorable because the large size of the aromatic group increases the steric hindrance among molecules.<sup>20</sup> On the other hand, the incorporation of an aromatic group could produce  $\pi$ - $\pi$  interactions among the adjacent aromatic groups. This  $\pi$ - $\pi$  interaction could influence the molecules to pack more compactly and then reduce the disadvantageous influence of steric hindrance to micellization.<sup>21–23</sup> In addition, the enhanced hydrophobicity derived from the incorporation of aromatic groups can also favor micelle formation.<sup>16,24</sup>

To expand the application of the *N*-aryl imidazolium ILs in the field of colloid and interface science, the aggregation behavior of three long-chain *N*-aryl imidazolium ILs in which the 2,4,6-trimethylphenyl group was grafted to the imidazolium ring was explored in the present work. The effect of the incorporation of the *N*-aryl moiety in the headgroup on micellization was investigated by surface tension, electrical conductivity, and <sup>1</sup>H NMR spectrometry. Compared with 1-alkyl-3-methylimidazolium salts, the incorporation of an aryl group has a significant influence on the surface activity, thermodynamics, and mechanism of micelle formation. In addition, the *N*-aryl imidazolium ILs have strong fluorescence properties that are due to the introduction of the aryl moiety.

## Experimental Section

**Materials.** 2,4,6-Trimethylaniline (98%), 1-bromododecane (98%), 1-bromotetradecane (98%), and 1-bromododecane (98%)

(15) Burns, C. T.; Lee, S.; Seifert, S.; Firestone, M. A. *Polym. Adv. Technol.* **2008**, *19*, 1369–1382.

(16) Dong, B.; Gao, Y. A.; Su, Y. J.; Zheng, L. Q.; Xu, J. K.; Inoue, T. *J. Phys. Chem. B* **2010**, *114*, 340–348.

(17) Yoshida, Y.; Baba, O.; Larriba, C.; Saito, G. *J. Phys. Chem. B* **2007**, *111*, 12204–12210.

(18) El Seoud, O. A.; Blaskó, A.; Bunton, C. A. *Langmuir* **1994**, *10*, 653–657.

(19) Okano, L. T.; El Seoud, O. A.; Halstead, T. K. *Colloid Polym. Sci.* **1997**, *275*, 138–145.

(20) Rózycka-Roszak, B. *J. Colloid Interface Sci.* **1990**, *140*, 538–540.

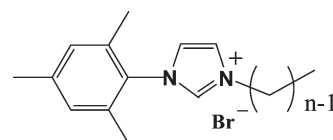
(21) Li, Y. J.; Reeve, J.; Wang, Y. L.; Thomas, R. K.; Wang, J. B.; Yan, H. K. *J. Phys. Chem. B* **2005**, *109*, 16070–16074.

(22) Yao, J. H.; Mya, K. Y.; Li, X.; Parameswaran, M.; Xu, Q. H.; Loh, K. P.; Chen, Z. K. *J. Phys. Chem. B* **2008**, *112*, 749–755.

(23) Chen, Q. B.; Liang, X. D.; Wang, S. L.; Xu, S. H.; Liu, H. L.; Hu, Y. *J. Colloid Interface Sci.* **2007**, *314*, 651–658.

(24) Fan, Y. R.; Li, Y. J.; Yuan, G. C.; Wang, Y. L.; Wang, J. B.; Han, C. C.; Yan, H. K.; Li, Z. X.; Thomas, R. K. *Langmuir* **2005**, *21*, 3814–3820.

**Chart 1. Chemical Structure of the ILs  $[\text{C}_n\text{pim}]\text{Br}$  ( $n = 10, 12$ , and 14)**



were purchased from Aladdin Chemical Reagent Co., Ltd.  $\text{D}_2\text{O}$  (99.96%) and  $\text{CDCl}_3$  (99.96%) were obtained from Sigma-Aldrich. Glyoxal (40%), MeOH (99.5%),  $\text{NH}_4\text{Cl}$  (99.5%), formaldehyde solution (37%), KOH (82%),  $\text{CH}_2\text{Cl}_2$  (99.5%),  $\text{H}_3\text{PO}_4$  (85%), tetrahydrofuran (99%), and toluene (99.5%) were purchased from Beijing Chemical Reagent Co. Triply distilled water was used throughout the experiments. The molecular structure of the ILs used in this work is depicted in Chart 1.

**Synthesis of 1-(2,4,6-Trimethylphenyl)imidazole.** 1-(2,4,6-Trimethylphenyl)imidazole was synthesized following a previously reported procedure.<sup>10</sup> Briefly, a mixture of aqueous glyoxal (0.1 m) and 2,4,6-trimethylaniline (0.1 m) in MeOH was stirred at room temperature until a yellow precipitate formed. After the addition of  $\text{NH}_4\text{Cl}$  (0.2 m), formaldehyde solution (37%, 0.21 m), and  $\text{H}_3\text{PO}_4$  (85%, 14 mL), the solution was refluxed for 9 h. The majority of the solvent (ca. 85%) was removed in vacuo, and then the pH of the solution was adjusted to 9 with KOH. The product was extracted with  $\text{CH}_2\text{Cl}_2$ , and then the solvent was removed in vacuo. The final product was purified by recrystallization using tetrahydrofuran at least four times. The purity of 2,4,6-trimethylaniline was ascertained by the <sup>1</sup>H NMR spectrum in  $\text{CDCl}_3$ .

**Synthesis of  $[\text{C}_n\text{pim}]\text{Br}$  ( $n = 10, 12$ , and 14).** For the synthesis of  $[\text{C}_{10}\text{pim}]\text{Br}$ , 2,4,6-trimethylphenylimidazole (0.1 mol, 18.6 g) and an excess amount of 1-bromododecane (0.11 mol, 24.3 g) were mixed in dry toluene (200 mL) in a 500 mL round-bottomed flask and then refluxed at 110 °C under a nitrogen atmosphere for 48 h. The obtained product was cooled to room temperature and purified by recrystallization in fresh diethyl ether at least four times. The final product was dried in vacuo for 48 h. The purity of  $[\text{C}_{10}\text{pim}]\text{Br}$  was ascertained by the <sup>1</sup>H NMR spectrum in  $\text{CDCl}_3$ .  $[\text{C}_{12}\text{pim}]\text{Br}$  and  $[\text{C}_{14}\text{pim}]\text{Br}$  were synthesized following the synthesis procedure for  $[\text{C}_{10}\text{pim}]\text{Br}$ .

**Apparatus and Procedures.** Surface tension measurements were carried out on a model JYW-200B tensiometer (Chengde Dahua Instrument Co., Ltd., accuracy  $\pm 0.1$  mN/m) using the ring method. Temperature was controlled at  $25 \pm 0.1$  °C using a thermostatic bath. All measurements were repeated until the values were reproducible.

Specific conductivity measurements on the aqueous solutions were performed using a low-frequency conductivity analyzer (model DDS-307, Shanghai Precision & Scientific Instrument Co., Ltd., accuracy  $\pm 1\%$ ).

<sup>1</sup>H NMR spectra were run on a Bruker Avance 400 spectrometer equipped with a pulse field gradient module (*Z* axis) using a 5 mm BBO probe. The instrument was operated at a frequency of 400.13 MHz at  $25 \pm 0.1$  °C. The observed chemical shifts ( $\delta_{\text{obs}}$ ) of the discrete protons of the ILs were examined as a function of concentration below and above the cmc. All of the samples were dissolved in  $\text{D}_2\text{O}$ , and chemical shifts were referenced to the center of the HDO signal (4.700 ppm). Two-dimensional nuclear overhauser effect spectroscopy (2D NOESY) was performed with the standard NOESY pulse sequence.<sup>25</sup> A relaxation delay of 2 s was used between scans. A sine apodization function ( $\text{ssb} = 2$ ) was applied in both dimensions before Fourier transformation. The mixing time was chosen to be 800 ms.

The fluorescence excitation and emission spectra were carried out using a PerkinElmer LS-55 spectrofluorometer (PE Company)

(25) Ernst, R. R.; Bodenhausen, G.; Wokaun, A. *Principles of Nuclear Magnetic Resonance in One and Two Dimensions*; Oxford University Press: New York, 1987.

equipped with a thermostatted cell holder at  $25 \pm 0.1$  °C. The slit widths were fixed at 10 and 3 nm for the excitation and emission, respectively.

## Results and Discussion

**Surface Properties and Micellization.** Surface tension measurements were performed to evaluate the surface activities of the three ILs in aqueous solutions. Figure 1 depicts the surface tension ( $\gamma$ ) versus concentration ( $C$ ) plots for the aqueous solutions of  $[C_n\text{pim}]\text{Br}$  ( $n = 10, 12, \text{ and } 14$ ) at 25 °C. The surface tension decreases initially with increasing concentration of  $[C_n\text{pim}]\text{Br}$ , suggesting that the IL molecules are adsorbed at the air/solution interface.<sup>26</sup> Then a plateau appears in the ( $\gamma$ - $C$ ) plot, indicating that the micelles have been formed, and the critical micelle concentration (cmc) is determined from the break point of the plot. The values of the cmc and  $\gamma_{\text{cmc}}$  (surface tension at cmc) for the three ILs are listed in Table 1, together with the data for 1-alkyl-3-methylimidazolium bromide,  $[C_n\text{mim}]\text{Br}$  ( $n = 10, 12, \text{ and } 14$ ).

Changes in the headgroup of the imidazolium ILs have an effect on their surface activities. As shown in Table 1, the cmc of  $[C_n\text{pim}]\text{Br}$  is much lower than that of  $[C_n\text{mim}]\text{Br}$  although they have the same alkyl chains, implying that the incorporated 2,4,6-trimethylphenyl group favors molecular aggregation. This is probably because the more delocalized charge of the cationic head reduces the electrostatic repulsion of the headgroups and thus facilitates micelle formation.<sup>27</sup> A similar result is obtained for  $[C_n\text{mim}]\text{Br}$  compared with traditional cationic surfactants (e.g., alkyltrimethylammonium bromides), where a lower cmc for  $[C_n\text{mim}]\text{Br}$  is due to the delocalized positive charge on the imidazolium ring.<sup>28</sup> The enhanced hydrophobicity derived from the incorporation of 2,4,6-trimethylphenyl groups can also be

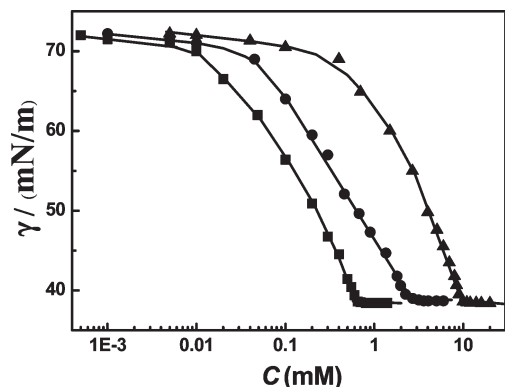


**Figure 1.** Surface tension of  $[C_n\text{pim}]\text{Br}$  aqueous solutions as a function of their concentrations.  $[C_{10}\text{pim}]\text{Br}$  ( $\blacktriangle$ ),  $[C_{12}\text{pim}]\text{Br}$  ( $\bullet$ ), and  $[C_{14}\text{pim}]\text{Br}$  ( $\blacksquare$ ) at 25 °C.

responsible for a decreased cmc. Because of the hydrophobic effect, the 2,4,6-trimethylphenyl group has a weak tendency to move away from the micellar interface, which means that the 2,4,6-trimethylphenyl group plays a role similar to that of the second hydrophobic chain when micelles are formed<sup>20</sup> and thus the cmc becomes smaller. This result is in agreement with the conclusion confirmed by  $^1\text{H}$  NMR spectra and 2D NOESY spectra as shown below. The  $\gamma_{\text{cmc}}$  value for  $[C_n\text{pim}]\text{Br}$  is also lower than that of  $[C_n\text{mim}]\text{Br}$ , suggesting that the former possesses a greater ability to reduce the surface tension. Herein, the surface activity of the novel *N*-aryl imidazolium ILs  $[C_n\text{pim}]\text{Br}$  is somewhat superior to that of *N*-alkyl imidazolium ILs  $[C_n\text{mim}]\text{Br}$  and the 2,4,6-trimethylphenyl group plays an important role in micelle formation.

The maximum excess surface concentration ( $\Gamma_{\text{max}}$ ) and the area occupied by a single amphiphile molecule at the air-water interface ( $A_{\text{min}}$ ), obtained from the Gibbs adsorption isotherm, can reflect the surface arrangement of surfactants at the air/liquid interface.<sup>29</sup> A greater value of  $\Gamma_{\text{max}}$  or a smaller value of  $A_{\text{min}}$  means a denser arrangement of surfactant molecules at the surface of the solution. It is clearly seen from Table 1 that  $[C_n\text{pim}]\text{Br}$  has a significantly larger  $\Gamma_{\text{max}}$  value and a correspondingly smaller  $A_{\text{min}}$  value than  $[C_n\text{mim}]\text{Br}$ , indicating a denser arrangement of  $[C_n\text{pim}]\text{Br}$  molecules at the air-water interface compared with that of  $[C_n\text{mim}]\text{Br}$ . This result is also caused by the more dispersed charge of the cations, which could weaken the electrostatic repulsion between headgroups. Moreover, the incorporation of a 2,4,6-trimethylphenyl group could produce  $\pi$ - $\pi$  interactions among the adjacent  $[C_n\text{pim}]\text{Br}$  molecules. This  $\pi$ - $\pi$  interaction could attract the molecules to pack more compactly in the air-water interface monolayer.<sup>23,24</sup>

The correlation between the cmc and the number of carbon atoms in the hydrocarbon chain ( $N_C$ ) for  $[C_n\text{pim}]\text{Br}$  is shown in Figure 2. The log cmc of  $[C_n\text{pim}]\text{Br}$  decreases linearly with the increase in  $N_C$ , following the empirical eq 1<sup>30</sup>

$$\log \text{cmc} = A - BN_C \quad (1)$$

where  $A$  and  $B$  are empirical constants. The value of  $A$  is related to the contribution of the polar head to micelle formation, and the value of  $B$  indicates the average contribution to the micelle formation by each methylene in the hydrophobic chain. Micelle formation is favored by smaller values of  $A$  or larger values of  $B$ .<sup>31</sup> The values of  $A$  and  $B$  for  $[C_n\text{pim}]\text{Br}$  calculated from Figure 2 are 0.89 and 0.29, respectively, which are different from those for  $[C_n\text{mim}]\text{Br}$ , where  $A = 1.05$  and  $B = 0.28$ .<sup>13</sup> This result indicates that the formation of micelles is much easier for  $[C_n\text{pim}]\text{Br}$  than for  $[C_n\text{mim}]\text{Br}$  in aqueous solution because of the incorporation of the 2,4,6-trimethylphenyl group.

**Thermodynamic Analysis of Micelle Formation.** The electrical conductivity of the IL aqueous solutions at different

**Table 1.** Surface Properties and Micellization Parameters of  $[C_n\text{pim}]\text{Br}$  ( $n = 10, 12, \text{ and } 14$ ) and  $[C_n\text{mim}]\text{Br}$  ( $n = 10, 12, \text{ and } 14$ ) in Aqueous Solutions at 25 °C

ILs	cmc (mM)			$\gamma_{\text{cmc}}$ (mN/m)	$\Gamma_{\text{max}}$ ( $\mu\text{mol}/\text{m}^2$ )	$A_{\text{min}}$ ( $\text{\AA}^2$ )
	determined from surface tension	determined from electrical conductivity	determined from $^1\text{H}$ NMR			
$[C_{10}\text{pim}]\text{Br}$	9.30	9.31	9.20	38.3	1.90	87.4
$[C_{12}\text{pim}]\text{Br}$	2.34	2.60	1.98	38.4	2.09	79.4
$[C_{14}\text{pim}]\text{Br}$	0.61	0.56		38.3	2.21	75.1
$[C_{10}\text{mim}]\text{Br}^a$	29.3	32.9	31	39.7	1.72	96.7
$[C_{12}\text{mim}]\text{Br}^a$	10.9	8.5	11	39.4	1.91	86.8
$[C_{14}\text{mim}]\text{Br}^b$	2.8	2.6		39.2	1.96	84.7

<sup>a</sup> Reported in refs 13 and 32. <sup>b</sup> Reported in ref 14.

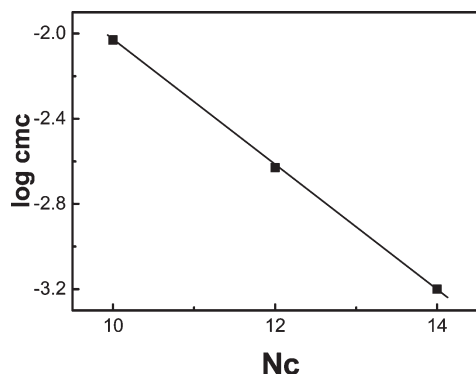


**Figure 2.** Logarithmic plots of cmc against the number of carbon atoms in the alkyl chain ( $N_C$ ) for  $[C_n\text{pim}]\text{Br}$  at 25 °C.

temperatures was measured to characterize the thermodynamics of micelle formation. The temperature dependence of electrical conductivity as a function of concentration for  $[C_n\text{pim}]\text{Br}$  ( $n = 10, 12,$  and  $14$ ) is shown in Figure 3. As the temperature increases, the cmc value of  $[C_n\text{pim}]\text{Br}$  increases, which is similar to the case for  $[C_n\text{mim}]\text{Br}$ .<sup>32</sup> The effect of temperature on the cmc of an ionic surfactant mainly includes two aspects.<sup>33</sup> A higher temperature reduces the degree of hydration of the hydrophilic headgroups, which facilitates micelle formation. Additionally, the water structures surrounding the hydrophobic chains are destroyed as the temperature increases, which hinders micelle formation. Because the cmc increases with temperature, it is clear that the latter effect plays a crucial role in micelle formation in these systems.

The degree of counterion binding ( $\beta$ ) can also be obtained from the electrical conductivity versus concentration plots on the basis of the mixed electrolyte model of micellar solution developed by Shanks and Franses.<sup>34</sup> The values of  $\beta$  for  $[C_n\text{pim}]\text{Br}$  at different temperatures are summarized in Table 2. Compared with  $[C_n\text{mim}]\text{Br}$ , with the same alkyl chain lengths (e.g.,  $\beta = 0.77$  ( $[C_{12}\text{mim}]\text{Br}$ )),<sup>32</sup> the present ILs,  $[C_n\text{pim}]\text{Br}$ , have a much lower value of  $\beta$ . The possible reason is that the interaction between the anion and hydrophilic group is reduced because of the larger size of the hydrophilic groups in the headgroup.<sup>20,35</sup>

As is well established in the thermodynamics of micelle formation, the standard Gibbs free energy of micelle formation ( $\Delta G_{\text{mic}}^0$ ) for ionic surfactants is given by eq 2<sup>36</sup>

$$\Delta G_{\text{mic}}^0 = (1 + \beta)RT \ln \chi_{\text{cmc}} \quad (2)$$

where  $\chi_{\text{cmc}}$  is the cmc in terms of the mole fraction. Once  $\Delta G_{\text{mic}}^0$  as a function of temperature is known, the standard enthalpy of

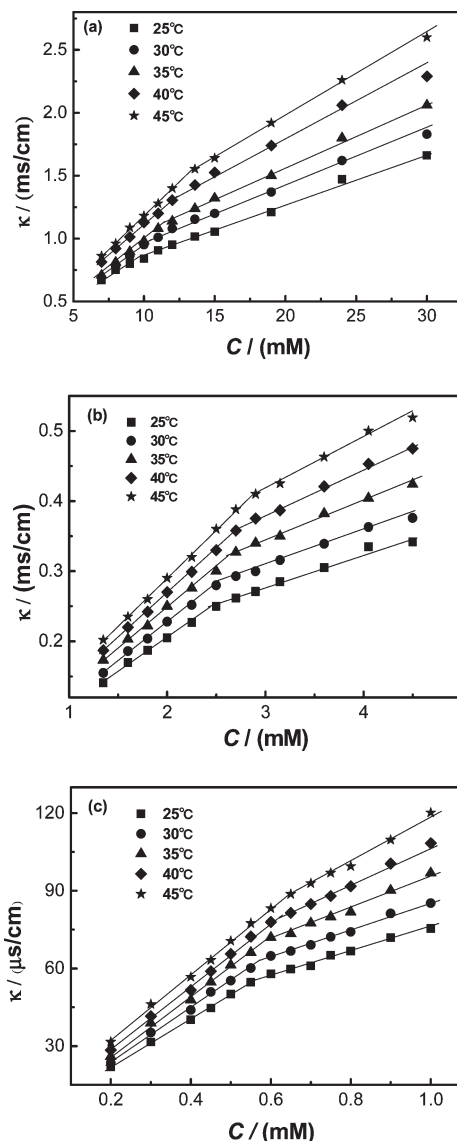


**Figure 3.** Specific conductivity as a function of concentration at different temperatures for (a)  $[C_{10}\text{pim}]\text{Br}$ , (b)  $[C_{12}\text{pim}]\text{Br}$ , and (c)  $[C_{14}\text{pim}]\text{Br}$ .

micelle formation ( $\Delta H_{\text{mic}}^0$ ) can be derived by applying the Gibbs–Helmholtz equation:

$$\left[ \frac{\partial(\Delta G_{\text{mic}}^0/T)}{\partial(1/T)} \right] = \Delta H_{\text{mic}}^0 \quad (3)$$

Then the standard entropy of micelle formation ( $\Delta S_{\text{mic}}^0$ ) is obtained through the following relation:

$$\Delta S_{\text{mic}}^0 = \frac{\Delta H_{\text{mic}}^0 - \Delta G_{\text{mic}}^0}{T} \quad (4)$$

The thermodynamic parameters for the ILs  $[C_n\text{pim}]\text{Br}$  ( $n = 10, 12,$  and  $14$ ) were thus obtained and are listed in Table 2.

The plots of  $\Delta G_{\text{mic}}^0$ ,  $\Delta H_{\text{mic}}^0$ , and  $-T\Delta S_{\text{mic}}^0$  as a function of temperature for  $[C_n\text{pim}]\text{Br}$  ( $n = 10, 12,$  and  $14$ ) are shown in Figure 4. In the range of temperatures investigated, the values of  $\Delta G_{\text{mic}}^0$  for the three ILs are negative and the negative  $\Delta G_{\text{mic}}^0$  values are mainly contributed by  $\Delta H_{\text{mic}}^0$ , suggesting that the micelle formation for the ILs in aqueous solution is enthalpy-driven. It is known

(26) Adamson, A. W.; Gast, A. P. *Physical Chemistry of Surfaces*, 6th ed.; Wiley-Interscience: New York, 1997.

(27) Miki, K.; Westh, P.; Nishikawa, K.; Koga, Y. *J. Phys. Chem. B* **2005**, *109*, 9014–9019.

(28) Zhang, H. C.; Li, K.; Liang, H. J.; Wang, J. J. *Colloids Surf., A* **2008**, *329*, 75–81.

(29) Jaycock, M. J.; Parfitt, G. D. *Chemistry of Interfaces*; John Wiley and Sons: New York, 1981.

(30) Shinoda, K. *Colloidal Surfactants: Some Physicochemical Properties*; Academic Press: New York, 1963; Chapter 1.

(31) Li, N.; Zhang, S. H.; Zheng, L. Q.; Dong, B.; Li, X. W.; Yu, L. *Phys. Chem. Chem. Phys.* **2008**, *10*, 1–3.

(32) Inoue, T.; Ebina, H.; Dong, B.; Zheng, L. Q. *J. Colloid Interface Sci.* **2007**, *314*, 236–241.

(33) Hunter, R. J. *Foundations of Colloid Science*; Oxford University Press: New York, 1989; Vol. 1.

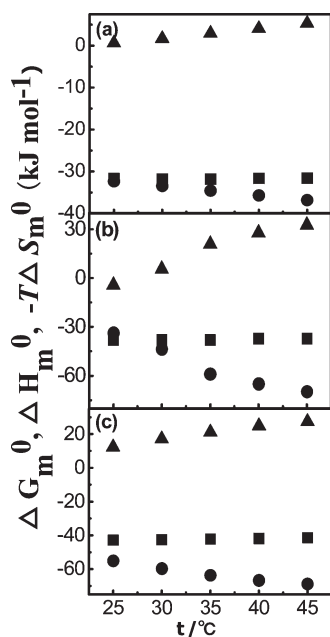
(34) Shanks, P. C.; Franses, E. I. *J. Phys. Chem.* **1992**, *96*, 1794–1805.

(35) Shimizu, S.; Pires, P. A. R.; El Seoud, O. A. *Langmuir* **2004**, *20*, 9551–9559.

(36) Stodghill, S. P.; Smith, A. E.; O'Haver, J. H. *Langmuir* **2004**, *20*, 11387–11392.

**Table 2. Critical Micelle Concentration (cmc), Degree of Counterion Binding ( $\beta$ ), and Thermodynamic Parameters of Micelle Formation for  $[C_n\text{pim}]\text{Br}$  ( $n = 10, 12, \text{ and } 14$ ) in Aqueous Solutions at Various Temperatures**

ILs	$T$ ( $^{\circ}\text{C}$ )	cmc (mM)	$\beta$	$\Delta G_m^0$ (kJ/mol)	$\Delta H_m^0$ (kJ/mol)	$-T\Delta S_m^0$ (kJ/mol)
$[C_{10}\text{pim}]\text{Br}$	25	9.8	0.48	-31.69	-32.3	0.61
	30	10.4	0.47	-31.79	-33.45	1.66
	35	11.2	0.46	-31.81	-34.56	2.96
	40	12.1	0.44	-31.60	-35.69	4.09
	45	13.3	0.43	-31.55	-36.84	5.29
$[C_{12}\text{pim}]\text{Br}$	25	2.61	0.54	-38.02	-33.75	-4.27
	30	2.67	0.52	-38.07	-43.56	5.49
	35	2.77	0.50	-38.05	-59.25	21.20
	40	2.84	0.47	-37.27	-65.64	28.37
	45	3.00	0.43	-37.15	-69.77	32.62
$[C_{14}\text{pim}]\text{Br}$	25	0.550	0.50	-42.74	-55.06	12.32
	30	0.574	0.47	-42.51	-59.68	17.17
	35	0.597	0.44	-42.18	-63.62	21.14
	40	0.624	0.40	-41.79	-66.62	24.83
	45	0.651	0.38	-41.41	-68.76	27.35

**Figure 4.** Thermodynamic parameters of aggregate formation as a function of temperature for (a)  $[C_{10}\text{pim}]\text{Br}$ , (b)  $[C_{12}\text{pim}]\text{Br}$ , and (c)  $[C_{14}\text{pim}]\text{Br}$  in water. Squares, circles, and triangles correspond to  $\Delta G_m^0$ ,  $\Delta H_m^0$ , and  $-T\Delta S_m^0$ , respectively.

that the enthalpy change of micellization is mainly contributed by hydrophobic and electrostatic interactions.<sup>37,38</sup> During micellization, the hydrocarbon chain of the surfactant monomer transfers from the aqueous environment to the micelle, accompanied by the release of solvating water molecules; this process is expected to be exothermic.<sup>39</sup> Electrostatic interactions are divided into self-repulsion of the headgroups and the counterions (exothermic) and attraction between the headgroup and the counterion (endothermic).<sup>35</sup> As mentioned above, the degree of counterion binding ( $\beta$ ) of the ILs  $[C_n\text{pim}]\text{Br}$  is rather low, suggesting that the self-repulsion of the headgroups and the counterions is stronger than the attraction between the headgroups and the counterions. That is, the contribution of electrostatic interactions should also be exothermic. Meanwhile, the effect of  $\pi$ - $\pi$  interactions arising

from the 2,4,6-trimethylphenyl group may be another reason for the large negative  $\Delta H_m^0$ , as observed for carbazole-tailed imidazolium ILs and phenyl-tailed surfactants.<sup>16,21,24</sup> Herein, it can be demonstrated that the 2,4,6-trimethylphenyl group introduced into the headgroup played an important role in micelle formation by the ILs.

**$^1\text{H}$  NMR Spectra.** It is known that prominent changes in both shielding and relaxation are presented in the NMR spectra during the aggregation of surfactants.<sup>40-42</sup> This means that proton signal changes can be obtained in both the hydrophobic chain and the hydrophilic group of a surfactant upon micellization. The proton assignments and  $^1\text{H}$  NMR spectra for  $[C_{10}\text{pim}]\text{Br}$  and  $[C_{12}\text{pim}]\text{Br}$  at different concentrations (below and above the cmc) in  $\text{D}_2\text{O}$  are shown in Figure 5a,b, respectively. ( $^1\text{H}$  NMR spectra for  $[C_{14}\text{pim}]\text{Br}$  were uninterpretable owing to its low cmc.) Discernible proton signals of the surfactant molecules in the  $^1\text{H}$  NMR spectra undergo obvious changes upon micellization. In particular, some small multiplets unite into broad ones ( $H_j$ ,  $H_k$ ), which is powerful evidence of the formation of thermodynamically stable self-assemblies.<sup>43</sup> The variation of the chemical shift of protons of  $[C_{10}\text{pim}]\text{Br}$ ,  $\Delta\delta$  ( $= \delta_{\text{obs}} - \delta_{\text{mon}}$ ), as a function of the reciprocal concentration is shown in Figure 6 as an example. Small changes in the chemical shifts are observed below the cmc, whereas above the cmc the chemical shifts change significantly. The sudden change in chemical shifts at the cmc may be caused by an abrupt change in the environment of the headgroup when micelles are formed; precisely, the configuration of the headgroup is adjusted to fit the critical packing parameter required for micelle formation.<sup>44</sup> A similar result was obtained for a chiral long-chain imidazolium IL, where the headgroup of the IL bends into the hydrophobic region during micellization.<sup>45</sup>

Protons in the present *N*-aryl imidazolium ILs could be divided into three classes: imidazole protons ( $H_a$ ,  $H_b$ ; no signal for  $H_c$  is observed because of the deuteration) and protons in the 2,4,6-trimethylphenyl group ( $H_d$ - $H_h$ ) and in the alkyl chain ( $H_i$ - $H_l$ ). It is clear in Figure 6 that protons of  $H_b$  and  $H_i$  move downfield

(40) Lindman, B.; Söderman, O.; Wennerström, H. In *Surfactant Solutions: New Methods of Investigation*; Zana, R., Ed.; Marcel Dekker: New York, 1987; Chapter 6.

(41) Nakagawa, T.; Tokiwa, F. In *Surface and Colloid Science*; Matijevic, E., Ed.; Wiley: New York, 1976; Vol. 9, p 69.

(42) Haigh, C. W.; Mallion, R. B. *Prog. Nucl. Magn. Reson. Spectrosc.* **1980**, *13*, 303-344.

(43) Singh, T.; Kumar, A. *J. Phys. Chem. B* **2007**, *111*, 7843-7851.

(44) Li, N.; Zhang, S. H.; Zheng, L. Q.; Inoue, T. *Langmuir* **2009**, *25*, 10473-10482.

(45) Li, X. W.; Gao, Y. A.; Liu, J.; Zheng, L. Q.; Chen, B.; Wu, L. Z.; Tung, C. H. *J. Colloid Interface Sci.* **2010**, *343*, 94-101.

(37) Myers, D. *Surfaces, Interfaces, and Colloids: Principles and Applications*, 2nd ed.; Wiley-VCH: New York, 1999.

(38) Muller, N. *Langmuir* **1993**, *9*, 96-100.

(39) Faucompré, B.; Bouzerda, M.; Lindheimer, M.; Douillard, J. M.; Partyka, S. *J. Therm. Anal.* **1994**, *41*, 1325-1333.

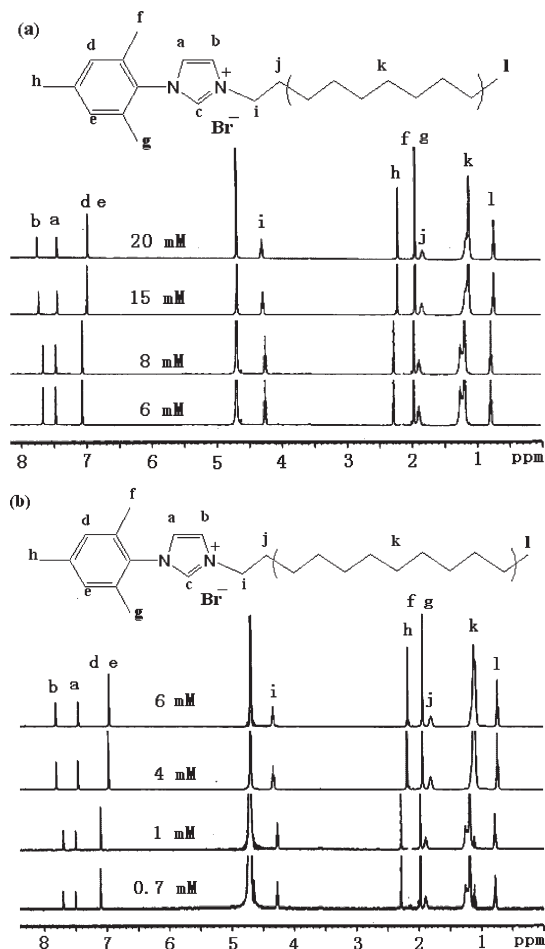


**Figure 5.** Proton assignments and  $^1\text{H}$  NMR spectra of (a)  $[\text{C}_{10}\text{pim}]\text{Br}$  and (b)  $[\text{C}_{12}\text{pim}]\text{Br}$  at concentrations below and above the cmc in  $\text{D}_2\text{O}$  at  $25\text{ }^\circ\text{C}$ .

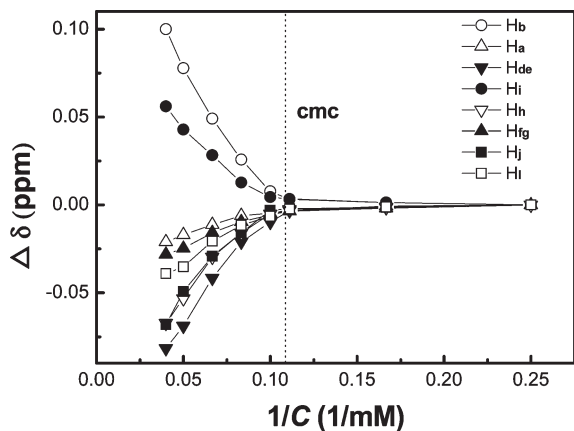


**Figure 6.** Variation of chemical shifts for various protons of  $[\text{C}_{10}\text{pim}]\text{Br}$  at different concentrations in  $\text{D}_2\text{O}$  at  $25\text{ }^\circ\text{C}$ .

whereas upfield shifts are exhibited for other protons. The chemical shifts upon micellization are mainly affected by the medium and conformational effects.<sup>46,47</sup> The medium effect is caused by the movement of surfactant molecules from water to micelles, where the hydrophobic chains of the surfactant molecules are

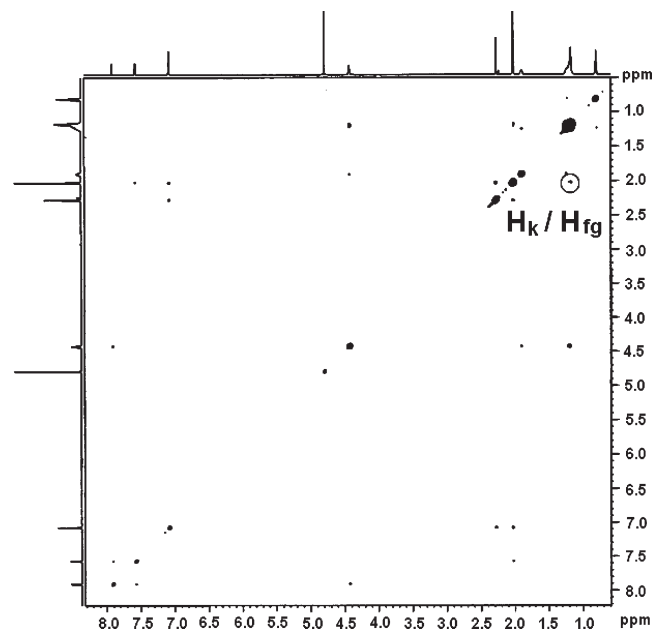


**Figure 7.** Two-dimensional NOESY spectra of  $[\text{C}_{10}\text{pim}]\text{Br}$  in  $\text{D}_2\text{O}$  at a concentration of  $40.0\text{ mM}$  at  $25\text{ }^\circ\text{C}$ .

immersed in a hydrophobic core and the hydrophilic headgroups are solvated by interfacial water molecules whose polarity is lower than that of bulk water. The decrease in the polarity of the micro-environment upon solvation leads to a downfield shift for the protons in the hydrophilic region.<sup>48</sup> The conformational effects, resulting from a partial changeover from a gauche to trans conformation in the alkyl chains upon micellization, usually make the protons in the middle of the hydrophobic chain shift downfield.<sup>49</sup> That is, in the absence of any other specific interaction that affects the observed chemical shift, one expects a downfield shift, as can be seen from  $\text{H}_b$  and  $\text{H}_i$ . The upfield shifts of other protons would be caused by the ring effect originating from the aromatic ring in the 2,4,6-trimethylphenyl group. It is known that protons located above and below the plane of the aromatic ring resonate at a higher field because of the shielding effect.<sup>50</sup> As the micelles are formed, the hydrophobicity of the 2,4,6-trimethylphenyl group makes it bend into the hydrophobic regions slightly, which causes the protons on the hydrophobic chains to move into the field of the ring current and then shift upfield. This result can be further verified by 2D NOESY. The 2D NOESY spectra of  $[\text{C}_{10}\text{pim}]\text{Br}$  in  $\text{D}_2\text{O}$  at a concentration of  $40.0\text{ mM}$  are provided in Figure 7, where a NOE contact between the protons in the 2,4,6-trimethylphenyl group ( $\text{H}_{f,g}$ ) and the hydrophobic chains ( $\text{H}_k$ ) is presented. The result suggests that the orientation of the 2,4,6-trimethylphenyl group is favorable in the hydrophobic region and the group interacts with the hydrophobic chains.

The protons of the 2,4,6-trimethylphenyl group ( $\text{H}_d\text{--H}_h$ ) shift upfield during micellization, which is in agreement with the result obtained above. As the 2,4,6-trimethylphenyl group bends into the hydrophobic regions upon micellization, the decrease in the polarity of the media in the hydrophobic regions could reduce the deshielding effect on the protons attached to the 2,4,6-trimethylphenyl group, which causes their upfield shifts.<sup>51</sup> In addition, the

(48) Tada, E. B.; Novaki, L. P.; El Seoud, O. A. *Langmuir* **2001**, *17*, 652–658.

(49) Persson, B. O.; Drakenberg, T.; Lindman, B. *J. Phys. Chem.* **1979**, *83*, 3011–3015.

(50) Shimizu, S.; El Seoud, O. A. *Langmuir* **2003**, *19*, 238–243.

(51) Fendler, J. H.; Fendler, E. J.; Infante, G. A.; Shih, P. S.; Patterson, L. K. *J. Am. Chem. Soc.* **1975**, *97*, 89–95.

(46) Huang, X.; Han, Y. C.; Wang, Y. X.; Wang, Y. L. *J. Phys. Chem. B* **2007**, *111*, 12439–12446.

(47) Persson, B. O.; Drakenberg, T.; Lindman, B. *J. Phys. Chem.* **1976**, *80*, 2124–2125.

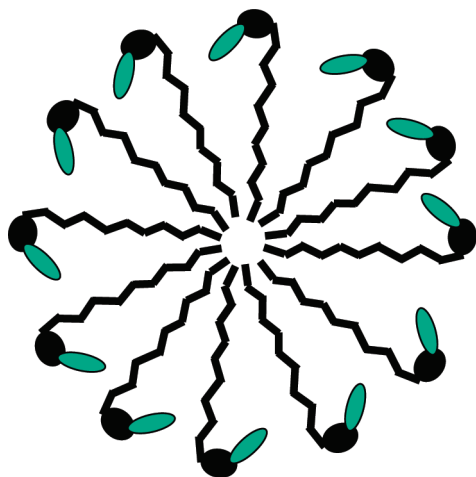


**Figure 8.** Schematic illustration of the proposed structures of micelles formed by  $[C_n\text{pim}]\text{Br}$  ( $n = 10$  as an example). Circles denote the imidazole rings; wavy lines denote the alkyl chains; and ellipses denote the 2,4,6-trimethylphenyl groups.

diamagnetic anisotropy of the  $\pi$ - $\pi$  conjugated system formed by the phenyl ring would bring about a remarkable shielding effect and thus lead to an upfield shift of the attached protons.<sup>16</sup> On the basis of theoretical calculations, Palomar<sup>52</sup> also believes that the chemical shift of the protons at the aromatic ring shifts downfield because of the specific interactions with water molecules whereas the nonspecific polarization effects of the solvent cage provide the opposite effect. According to the analysis above, a possible packing structure of molecules in the micelle is depicted in Figure 8. In this staggered arrangement, the 2,4,6-trimethylphenyl group tends to move away from the micellar interface and then bend into the hydrophobic region to a small extent.

Interestingly, an upfield shift is observed for the other proton on the imidazolium ring ( $H_a$ ). Competition between the medium effect and the phenyl-group-induced ring-current effect could be responsible for the result. As the 2,4,6-trimethylphenyl group is inserted, the aromatic-moiety-induced magnetic deshielding effect on  $H_a$  is more significant when compared to the hydrogen-bonding interaction between  $H_a$  and interfacial water molecules. When the micelles are formed, the deshielding effect is reduced by the decreased polarity, which causes an upfield shift for  $H_a$ .

The cmc for surfactants can also be obtained from the  $^1\text{H}$  NMR chemical shifts.<sup>53</sup> On the basis of the fast exchange of the surfactant molecules on the NMR timescale, the observed chemical shift ( $\delta_{\text{obs}}$ ) can be expressed as a weighted average of the chemical shifts of the monomer ( $\delta_{\text{mon}}$ ) and the micelle ( $\delta_{\text{mic}}$ )

$$\delta_{\text{obs}} = \delta_{\text{mon}} \left( \frac{C_{\text{mon}}}{C_{\text{T}}} \right) + \delta_{\text{mic}} \left( \frac{C_{\text{mic}}}{C_{\text{T}}} \right) \quad (5)$$

where  $C_{\text{mon}}$ ,  $C_{\text{mic}}$ , and  $C_{\text{T}}$  are the concentrations of surfactant existing as monomers, micelles, and the total concentration, respectively. It is assumed that the monomer concentration is constant above the cmc, thus

$$\delta_{\text{obs}} = \delta_{\text{mic}} - \left( \frac{\text{cmc}}{C_{\text{T}}} \right) (\delta_{\text{mic}} - \delta_{\text{mon}}) \quad (6)$$

$\delta_{\text{mon}}$  and  $\delta_{\text{mic}}$  can be estimated by extrapolation of the plots of  $\delta_{\text{obs}}$  versus  $C_{\text{T}}$  and  $\delta_{\text{obs}}$  versus  $1/C_{\text{T}}$ , respectively. Figure 9 shows

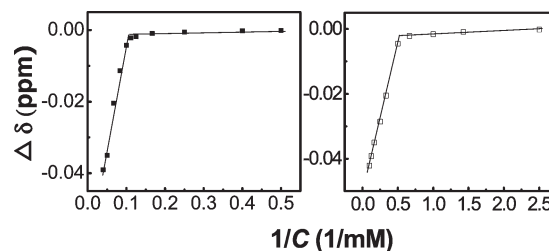


**Figure 9.** Variation of chemical shifts for the terminal proton ( $H_1$ ) signals vs the reciprocal concentration of  $[C_{10}\text{pim}]\text{Br}$  (left) and  $[C_{12}\text{pim}]\text{Br}$  (right) in  $\text{D}_2\text{O}$  at  $25^\circ\text{C}$ .

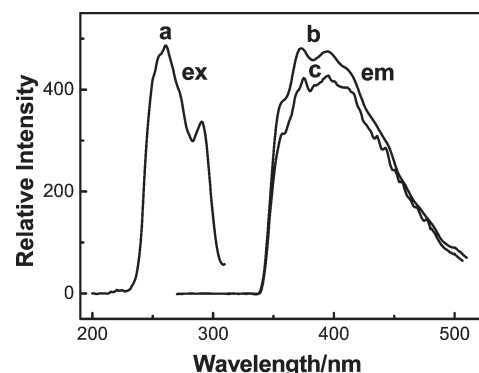


**Figure 10.** (a) Excitation and (b, c) emission spectra of  $[C_{10}\text{pim}]\text{Br}$  in aqueous solutions with a concentration of  $2.0\text{ mmol/L}$ .  $\lambda_{\text{em}}$  (nm): (a)  $370$ .  $\lambda_{\text{ex}}$  (nm): (b)  $290$  and (c)  $260$ .

an example of the variation of chemical shifts ( $\delta_{\text{obs}} - \delta_{\text{mon}}$ ) versus  $1/C_{\text{T}}$  plots for the terminal protons ( $H_1$ ) of  $[C_{10}\text{pim}]\text{Br}$  and  $[C_{12}\text{pim}]\text{Br}$ . It can be seen that two straight lines were obtained and the intersection point corresponds to the cmc ( $9.20\text{ mM}$  for  $[C_{10}\text{pim}]\text{Br}$ ,  $1.98\text{ mM}$  for  $[C_{12}\text{pim}]\text{Br}$ ), which is a little lower than that in  $\text{H}_2\text{O}$  because  $\text{D}_2\text{O}$  is a more structured liquid.<sup>54</sup>

**Fluorescence Properties.** The fluorescence properties of  $[C_n\text{pim}]\text{Br}$  ( $n = 10, 12,$  and  $14$ ) in aqueous solution were measured at various concentrations. Figure 10 shows the excitation and emission spectra for aqueous solutions of  $[C_{10}\text{pim}]\text{Br}$  at a concentration of  $2.0\text{ mmol/L}$ . It can be seen that strong fluorescence peaks are present in both the excitation and emission spectra. Notably, when excited at different excitation wavelengths, the emission peak position remains unchanged, suggesting that the  $N$ -aryl imidazolium ILs have stable, strong fluorescence. It is known that most traditional imidazolium ILs are not fluorescent.<sup>55,56</sup> Thus, the fluorescence of the new ILs is ascribed to the incorporation of the 2,4,6-trimethylphenyl group. The unique fluorescence properties of the ILs may extend their application into the field of photochemistry.

## Conclusions

The aggregation behavior of three  $N$ -aryl imidazolium ILs  $[C_n\text{pim}]\text{Br}$  ( $n = 10, 12,$  and  $14$ ) in aqueous solutions was investigated by surface tension, electrical conductivity, and  $^1\text{H}$  NMR. The cmc obtained for  $[C_n\text{pim}]\text{Br}$  is much lower than that for  $[C_n\text{mim}]\text{Br}$ , suggesting that the incorporation of the 2,4,6-trimethylphenyl group facilitates micelle formation. The prominently enhanced  $\pi$ - $\pi$  interactions due to the 2,4,6-trimethylphenyl

(52) Palomar, J.; Ferro, V. R.; Gilarranz, M. A.; Rodriguez, J. J. *J. Phys. Chem. B* **2007**, *111*, 168–180.

(53) Goon, P.; Das, S.; Clemett, C. J.; Tiddy, T.; Kumar, V. V. *Langmuir* **1997**, *13*, 5577–5582.

(54) Chang, N. J.; Kaler, E. W. *J. Phys. Chem.* **1985**, *89*, 2996–3000.

(55) Paul, A.; Mandal, P. K.; Samanta, A. *Chem. Phys. Lett.* **2005**, *402*, 375–379.

(56) Paul, A.; Mandal, P. K.; Samanta, A. *J. Phys. Chem. B* **2005**, *109*, 9148–9153.

groups cause the  $[C_n\text{pim}]\text{Br}$  molecules to arrange densely at the air–water interface. The thermodynamic results revealed that the micelle formation for  $[C_n\text{pim}]\text{Br}$  ( $n = 10, 12, \text{ and } 14$ ) is enthalpy-driven throughout the whole temperature range (25–45 °C), which is attributed to strong self-repulsion of the headgroups and counterions and  $\pi$ – $\pi$  interactions among the 2,4,6-trimethylphenyl groups in the micelles. The results of  $^1\text{H}$  NMR and 2D NOESY spectra indicate that the 2,4,6-trimethylphenyl group slightly bends into the hydrophobic region when micelles are

formed. These *N*-aryl imidazolium ILs present strong, stable fluorescence properties, which could extend their applications in optical fields.

**Acknowledgment.** We thank the National Natural Science Foundation of China (nos. 20773081 and 50972080) and the National Basic Research Program (2009CB930101) for financial support and Dr. Pamela Holt (Shandong University) for proof-reading the manuscript.